bioRxiv preprint doi: https://doi.org/10.1101/2021.07.22.453374; this version posted July 22, 2021. The copyright holder for this preprint (which was not certified by peer review) is the author/funder, who has granted bioRxiv a license to display the preprint in perpetuity. It is made available under aCC-BY 4.0 International license.

Numerical approaches for the rapid analysis of prophylactic efficacy against HIV with arbitrary drug-dosing schemes

Lanxin Zhang[1], Junyu Wang[1], Max von Kleist[1],

1 Project group 5 "Systems Medicine of Infectious Disease", Robert Koch Institute, Berlin, Germany

* kleistm@rki.de

Abstract

Pre-exposure prophylaxis (PrEP) is an important pillar to prevent HIV transmission. Because of experimental and clinical shortcomings, mathematical models that integrate pharmacological, viral- and host factors are frequently used to quantify clinical efficacy of PrEP. Stochastic simulations of these models provides sample statistics from which the clinical efficacy is approximated. However, many stochastic simulations are needed to reduce the associated sampling error. To remedy the shortcomings of stochastic simulation, we developed three numerical methods that allow predicting the efficacy of arbitrary prophylactic regimen directly from a viral dynamics model, without sampling. We apply the methods to various hypothetical dolutegravir (DTG) prophylaxis scenarios. The approaches are verified against one another, as well as state-of-the-art stochastic simulation. While the methods are more accurate than stochastic simulation, they are superior in terms of computational performance. For example, a continuous 6-month prophylactic profile is computed within a few seconds on a laptop computer. The methods' computational performance, therefore, substantially expands the horizon of feasible analysis in the context of PrEP, and possibly other applications.

Author summary

Pre-exposure prophylaxis (PrEP) is an important tool to prevent HIV transmission. However, experimental identification of parameters that determine prophylactic efficacy is extremely difficult. Clues about these parameters could prove essential for the design of next-generation PrEP compounds. Integrative mathematical models can fill this void: Based on stochastic simulation, a sample statistic can be generated, from which the prophylactic efficacy is estimated. However, for this sample statistic to be accurate, many simulations need to be performed.

Here, we introduce three numerical methods to directly compute the prophylactic efficacy from a viral dynamics model, without the need for sampling. Based on several examples with dolutegravir (DTG) -based short- and long-term PrEP, as well as post-exposure prophylaxis we demonstrate the correctness of the new methods and their outstanding computational performance. Due to the methods' computational performance, a number of analysis, including formal sensitivity analysis are becoming feasible with the proposed methods.

bioRxiv preprint doi: https://doi.org/10.1101/2021.07.22.453374; this version posted July 22, 2021. The copyright holder for this preprint (which was not certified by peer review) is the author/funder, who has granted bioRxiv a license to display the preprint in perpetuity. It is made available under aCC-BY 4.0 International license.

Introduction

Since its transfer to human in the early 20th century [1], HIV remains a major public health treat. According to UNAIDS estimates, approximately 38 million individuals worldwide are infected with the human immunodeficiency virus (HIV) [2]. HIV continues to spread and the latest incidence estimates amount to about 1.7 million new infections in 2019 [2]. Sub-Saharan Africa is hit hardest by the HIV pandemic, and due to COVID many services, including HIV control and treatment, had been suspended, which could lead to a long-term re-surge in infections [3].

Nowadays, about 30 antiviral compounds are available that can stop HIV replication and prevent the acquired immunodeficiency symdrome (AIDS) and AIDS-related death [4]. However, unlike many other infections, no cure is available to clear HIV, which can persist in latent reservoirs for decades [5, 6]. Available treatments therefore have to be taken life-long to prevent the relapse of virus from latent reservoirs and to prevent AIDS. As a consequence, much focus around fighting HIV turned towards HIV prevention. While a vaccine would be the ideal tool for the purpose, intrinsic difficulties have so far precluded the development of an effective vaccine against HIV [7]. However, based on the successes in antiviral drug discovery, recent years have seen an increasing interest in utilising antivirals not only for treatment, but also to prevent HIV transmission. Two general strategies are currently implemented for this purpose: (i) Treatment-as-prevention (TasP) intends to put individuals with an HIV diagnosis immediately on treatment, which essentially makes them non-contagious by decreasing the number of viruses they can expose to uninfected individuals [8]. (ii) Pre-exposure prophylaxis (PrEP) on the other hand prevents establishment of HIV infection after exposure [9, 10].

Currently, two oral PrEP options, the patent-expired two-compound combination Truvada, as well as the patent-protected two-compound combination Descovy are available. However, many more drugs are investigated for re-purposing [11, 12], or under *de novo* development [13], including topically-applied drugs, long-acting injectibles, as well as drug eluting implants [14] [15].

However, demonstrating clinical efficacy of novel PrEP compounds constitutes a formidable task. Clinical efficacy of PrEP is understood as the reduction in the number of infected individuals in a treatment- vs. a control arm of a clinical trial [9]. A major statistical problem arises from the fact that HIV transmission probabilities are extremely low (e.g. $< 3\%$ during unprotected sex [16]; far less for condom- or PrEP usage, and when potential transmitters take antiviral therapy). Hence, the number of evaluable data points (= infected individuals in a trial treatment and control arm) are extremely low and prone to chance events. Since the approval of Truvada-based PrEP, novel PrEP interventions have to be compared with Truvada, worsening the statistical problem considerably [17]. E.g. the recent DISCOVER trial evaluating the efficacy of emtricitabine plus tenofovir alafenamide (Descovy) against Truvada was conducted over 8756 person-years [10], yielding as little as 22 evaluable data points (infections). Statistically empowering such a study quickly exceeds organizational and monetary capacities. The statistical limitation has two consequences: (a) The determination of concentration-prophylaxis relations, threshold concentrations and contributions of transmitted and acquired drug-resistance cannot be rigorously deduced from clinical data, non-withstanding ethical concerns. (b) The hurdles to introduce next-generation PrEP regimen are immense: Trials consume huge monetary resources and require several years. This compromises the advancement of next-generation PrEP and likely affects its costs. It is therefore absolutely crucial to discern promising from less promising interventions *a priori*.

Auxiliary tools based on integrative mathematical modelling may help to better understand the parameters contributing to clinical PrEP efficacy [18]. In particular,

bioRxiv preprint doi: https://doi.org/10.1101/2021.07.22.453374; this version posted July 22, 2021. The copyright holder for this preprint (which was not certified by peer review) is the author/funder, who has granted bioRxiv a license to display the preprint in perpetuity. It is made available under aCC-BY 4.0 International license.

how drug dosing may alter the risk of acquiring HIV infection, depending on its timing and the magnitude of viral exposure.

A key feature of HIV biology is that transmission is highly inefficient. For example, $< 3\%$ of unprotected sex acts between sero-discordant partners result in HIV infection [16]. Moreover, the number of genetically distinct founder viruses is extremely low [19]. This argues that stochastic processes play an important role during early infection, and that, in the majority of exposures, the virus becomes eliminated before it irreversibly infects the new host. Therefore, stochastic modelling and simulation approaches are used to estimate the efficacy of PrEP by integrating various host-, viral- and drug-specific parameters. For fixed drug concentrations, Monte-Carlo schemes, analytical, as well as probability generating ODE systems have been developed [20–22]. These approaches have been extended to include time-varying drug concentrations by integrating pharmacokinetic characteristics, as well as realistic dosing schemes, but were restricted to particular drugs, drug classes or prophylactic schemes [23, 24]. Recently, a numerically exact Monte-Carlo approach was introduced that can be universally applied to study the effects of dosing, pharmacokinetics, drug adherence, timing and extend of viral exposure on the risk of HIV infection [11, 12]. Despite its advantage, the introduced stochastic simulation approach is still computationally prohibitive, in a sense that it would not allow to compute a PrEP efficacy from a history of drug dosing 'on the fly', e.g. to be useful in a health app or computer program that empowers PrEP users, akin to [25].

In this work, we derive three numerical methods from an established viral dynamics model of HIV infection [26, 27] that overcome aforementioned limitations. These methods estimate the probability of viral extinction using a set of low-dimensional deterministic Ansatz functions that are either solved iteratively or with standard numerical solvers. The fastest of the three methods allows to quantify PrEP efficacy within fractions of a second on a standard computer and is numerically exact up to the tolerance level of an ODE-solver. All developed methods fully integrate drug pharmacokinetics, which allows to estimate the influence of drug dosing, drug adherence, timing and magnitude of viral exposure on PrEP efficacy.

We illustrate the methods with the second-generation integrase inhibitor dolutegravir (DTG). Taking advantage of the outstanding performance of the developed methods, we presented several show cases to display their possible applications: By estimating (i) both pre- and post-exposure prophylaxis with different dosing of the drug, as well as timing- and extent of virus exposure, (ii) prophylactic protection profiles over a 6 month dosing history, as well as (iii) timing- and probability of viral establishment with different exposures.

Methods

Below, we will introduce a within-host HIV dynamics model, as well as a pharmacokinetic-pharmacodynamic model of the second-generation integrase dolutegravir, which serve as a common basis to derive and demonstrate the presented numerical methods to compute HIV prophylactic efficacy. We will then introduce the three proposed methods: Next Transition Method (NTM), Constant Time Step Method (CTSM) and the Probability Generating System (PGS). A formal derivation of the methods can be found in Supplementary Text S1. Pseudo-codes for the respective methods are found in Supplementary Texts S2-4. In Supplementary Text S5 the equations for each method are derived in the case where the model is extended for long-lived and latently infected cells. While the second- (CTSM) and third- (PGS) method are related, in Supplementary Text S6 we show how to derive the third method (PGS) from the first (NTM).

bioRxiv preprint doi: https://doi.org/10.1101/2021.07.22.453374; this version posted July 22, 2021. The copyright holder for this preprint (which was not certified by peer review) is the author/funder, who has granted bioRxiv a license to display the preprint in perpetuity. It is made available under aCC-BY 4.0 International license.

HIV viral dynamics model

We adapted the viral dynamics model from [26,27]. We use this model, because it allows to mechanistically integrate the mechanisms of action of all approved drugs (and drug classes) [26] and because it allows to integrate both drug-specific *in vitro* and *in vivo* parameters [24]. In its most basic form, the considered viral replication cycle consists of free infectious viruses V, early infected T-cells (T_1), and productively infected T-cells (T_2). The dynamics can be defined by six reactions R_1 to R_6 with propensities a_{1-6}:

$$\begin{aligned}
&R_1: \text{Clearance of free virus,} && V \to * && a_1 = (CL + CL_T \cdot T_u) \cdot V && (1)\\
&R_2: \text{Clearance of } T_1\text{-cell,} && T_1 \to * && a_2 = (\delta_{PIC} + \delta_{T_1}) \cdot T_1 && (2)\\
&R_3: \text{Clearance of } T_2\text{-cell,} && T_2 \to * && a_3 = \delta_{T_2} \cdot T_2 && (3)\\
&R_4: \text{Infection of a suscept. cell,} && V \to T_1 && a_4 = \beta \cdot T_u \cdot V && (4)\\
&R_5: \text{Integration of viral DNA,} && T_1 \to T_2 && a_5(\varnothing) = k \cdot T_1 && (5)\\
&R_6: \text{Production of new virus,} && T_2 \to V + T_2 && a_6 = N_T \cdot T_2, && (6)
\end{aligned}$$

where we assume that the integrase inhibitor dolutegravir (DTG) inhibits proviral genome integration (reaction R_5), with details outlined below. Moreover, we assume that a T_2-cell continuously produces viruses (with reaction rate R_6) until it is cleared (continuous virus production model). The basic model is depicted in Fig 1. Utilized model parameters and their interpretations are given in Table 1.

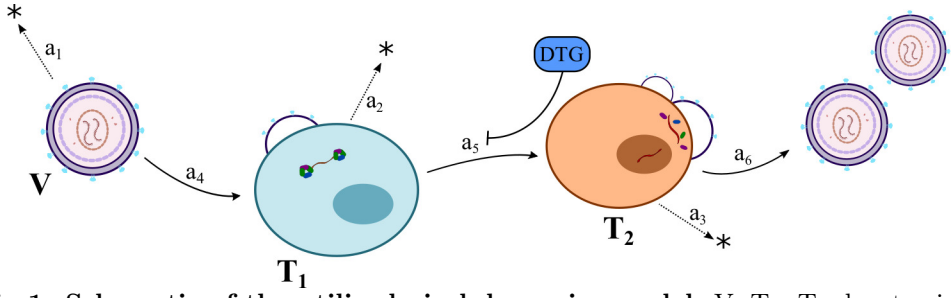

Fig 1. Schematic of the utilized viral dynamics model. V, T_1, T_2 denote virus, early infected T-cells and productively infected T-cells respectively. Each reaction is denoted by its reaction propensity $a_1 - a_6$. Briefly, a free virus can either be cleared (with reaction propensity a_1), or infect a susceptible T cell with rate a_4 to yield an early infected cell T_1. These cells denote a state where the virus has penetrated the host cell, but has not yet integrated its proviral DNA into the host cell's genome, thus not yet producing viral offspring. Early infected cell T_1 can either be cleared with rate a_2 or the proviral DNA irreversibly become integrated into the host cells DNA with rate a_5 to yield a productively infected T-cell T_2. T_2 cells start producing infectious progeny virus with rate a_6, or they may get cleared by the immune system with rate a_3.

Pharmacokinetics and pharmacodynamics of dolutegravir

Dolutegravir (DTG) is a second-generation integrase inhibitor which may potentially be used as prophylaxis against HIV. Moreover, we study it because of its similarity to carbotegravir, which is in clinical development as a next-generation PrEP compound. To evaluate the PrEP utility of DTG, we utilize a previously developed pharmacokinetic-pharmacodynamic model of the drug [11].

bioRxiv preprint doi: https://doi.org/10.1101/2021.07.22.453374; this version posted July 22, 2021. The copyright holder for this preprint (which was not certified by peer review) is the author/funder, who has granted bioRxiv a license to display the preprint in perpetuity. It is made available under aCC-BY 4.0 International license.

Table 1. Parameters for viral dynamics model.

Parameter	Description	Value	Reference
CL	clearance rate of free virus by the immune system	2.3	[28, 29]
CL_{T}	clearance rate of the free virus during unsuccessful infection	$CL_{\mathrm{T}} = \left(\frac{1}{\rho_{rev}} - 1\right) \cdot \beta$	[26]
T_u	level of uninfected T-cells in the disease-free state	$T_u = \lambda_{\mathrm{T}}/\delta_{\mathrm{T}}$	
ρ_{rev}	probability of successful reverse transcription	0.5	[30, 31]
β	lumped rate of infection of T-cells	$8 \cdot 10^{-12}$	[32]
λ_{T}	birth rate of uninfected T-cells	$2 \cdot 10^{9}$	[33]
δ_{T}	death rate of uninfected T-cells	0.02	[34]
δ_{PIC}	rate of intracellular destruction of pre-integration complex (PIC);	0.35	[31, 35]
δ_{T_1}	rate of clearance of T_1-cells	0.02	[34]
δ_{T_2}	rate of clearance of T_2-cells	1	[36]
k	rate by which T_1-cells are transformed into T_2-cells	0.35	[31]
N_{T}	rate of production of infectious progeny virus	670	[26, 34]

All parameters are in units [1/day], except for λ [cells/day] and β [1/(day·virus)]

Pharmacokinetics of dolutegravir

We utilize the non-linear mixed effects pharmacokinetic model introduced in [11]. In brief, a two-compartment model with first order absorption describes the plasma concentrations time profiles of dolutegravir (DTG) after oral drug administration. Individual parameters for a population of HIV-negative individuals were sampled from the distributions defined in [11] (Table 2 therein). The structural pharmacokinetic model is given by the following set of ordinary differential equations (ODEs):

$$\frac{d}{dt}Z_1 = -k_a \cdot Z_1 \tag{7}$$

$$\frac{d}{dt}D = \frac{d}{dt}Z_2 = \frac{k_a}{V_c/F_{bio}} \cdot Z_1 - \frac{CL/F_{bio}}{V_c/F_{bio}} \cdot Z_2 - \frac{Q/F_{bio}}{V_c/F_{bio}} \cdot Z_2 + \frac{Q/F_{bio}}{V_p/F_{bio}} \cdot Z_3 \tag{8}$$

$$\frac{d}{dt}Z_3 = \frac{Q/F_{bio}}{V_c/F_{bio}} \cdot Z_2 - \frac{Q/F_{bio}}{V_p/F_{bio}} \cdot Z_3 \tag{9}$$

where Z_1 represents the amount of drug in the dosing compartment, and Z_3 denotes the DTG concentration in the peripheral compartment. $D = Z_2$ is the DTG concentration in the blood plasma, i.e. the value of interest. In a therapy, the value Z_1 increases whenever a dosing event τ_k occurs: $Z_{1,t} = Z_{1,t} + \mathrm{dose_k}$.

Pharmacodynamics of DTG

Since DTG is an integrase inhibitor, it acts intracellularly by preventing the integration of viral DNA. This effect can be translated into a decrease in propensity function a_5 by a factor $1 - \eta_D$

$$a_5(t) = (1 - \eta_D(t)) \cdot k \cdot T_1 \tag{10}$$

where $\eta_D(t)$ denotes the direct effect of DTG at time t, which is modelled using the Emax-equation [37]:

$$\eta_D(t) = \frac{D_t^m}{IC_{50}^m + D_t^m} \tag{11}$$

where D_t is the drug concentration in the blood plasma at time t. IC_{50} represents the plasma drug concentration by which the activity of proviral integration is inhibited by 50%, and m denotes a hill coefficient. In this work $IC_{50} = 89$ [nM] and $m = 1.3$ is used, which are values after protein adjustment [38] (free drug hypothesis).

bioRxiv preprint doi: https://doi.org/10.1101/2021.07.22.453374; this version posted July 22, 2021. The copyright holder for this preprint (which was not certified by peer review) is the author/funder, who has granted bioRxiv a license to display the preprint in perpetuity. It is made available under aCC-BY 4.0 International license.

Prophylactic efficacy

The prophylactic efficacy φ is defined as the reduction of infection risk for a prophylactic regimen $\mathcal{S}$, compared to the infection probability in the absence of prophylaxis:

$$\varphi(Y_t, \mathcal{S}) = 1 - \frac{P_I(Y_t, \mathcal{S})}{P_I(Y_t, \varnothing)} \tag{12}$$

where $P_I(Y_t, \mathcal{S})$ and $P_I(Y_t, \varnothing)$ denote the infection probabilities in the presence and absence of a prophylactic regimen $\mathcal{S}$ for a given virus state (e.g. exposure) Y_t at time t. We consider a prophylactic regimen to be a continuous function of drug concentrations. The state of the viral compartments Y_t is defined as $Y_t = [V, T_1, T_2]^T$, where V, T_1 and T_2 are the numbers of viruses, T_1-cells and T_2-cells, respectively. For the absence of prophylaxis, $P_I(Y_t, \varnothing)$, analytical solutions have been presented in [38]. For a prophylactic regimen $\mathcal{S}$ they need to be determined numerically.

The infection probability is the complement of the extinction probability P_E. We thus have

$$P_I(Y_t, \mathcal{S}) = 1 - P_E(Y_t, \mathcal{S}) \tag{13}$$

where

$$P_E(Y_t) := \mathbb{P}\left(Y_\infty = \begin{bmatrix} 0 \\ 0 \\ 0 \end{bmatrix} \;\middle|\; Y_t = \begin{bmatrix} V \\ T_1 \\ T_2 \end{bmatrix} \right).$$

In words, the probability that all viral compartments will eventually go extinct, starting from state Y_t at time t. Under the reasonable assumption of statistical independence, akin to [38], we can define the extinction probability as:

$$P_E\left(Y_t, \mathcal{S}\right) = \left(P_E(\hat{V}, \mathcal{S})\right)^V \cdot \left(P_E(\hat{T_1}, \mathcal{S})\right)^{T_1} \cdot \left(P_E(\hat{T_2}, \mathcal{S})\right)^{T_2} \tag{14}$$

where $\hat{V}, \hat{T_1}, \hat{T_2}$ represent the unit vectors:

$$\hat{V} = \begin{bmatrix} 1 \\ 0 \\ 0 \end{bmatrix},\ \hat{T_1} = \begin{bmatrix} 0 \\ 1 \\ 0 \end{bmatrix},\ \hat{T_2} = \begin{bmatrix} 0 \\ 0 \\ 1 \end{bmatrix} \tag{15}$$

Thus, if $P_E(\hat{V}, \mathcal{S}), P_E(\hat{T_1}, \mathcal{S})$ and $P_E(\hat{T_2}, \mathcal{S})$ can be determined, the prophylactic efficacy can also be calculated using eq (12)–(14),

Low-dimensional deterministic Ansatz functions

In this section, we present three methods to compute the extinction probability for the unit vectors $P_E(\hat{V}, \mathcal{S}), P_E(\hat{T_1}, \mathcal{S})$ and $P_E(\hat{T_2}, \mathcal{S})$, which enable the integration of arbitrary pharmacokinetic profiles resulting from some prophylactic regimen $\mathcal{S}$. As noted before, this would enable calculating prophylactic efficacy for arbitrary drug/dosing regimen.

Distribution of state transition events

The viral dynamic model illustrated in Fig. 1 is interpreted as a continuous time, discrete state Markov process [39]. Therefore, the time when a particular state transition happens is exponentially distributed according to the reaction propensities. In the viral replication cycle, if the initial state is $Y_0 = [1, 0, 0]^T$, there are two possible next states: (i) the virus is cleared $Y_\tau = [0, 0, 0]^T$, or a T_1-cell emerges $Y_\tau = [0, 1, 0]^T$,

bioRxiv preprint doi: https://doi.org/10.1101/2021.07.22.453374; this version posted July 22, 2021. The copyright holder for this preprint (which was not certified by peer review) is the author/funder, who has granted bioRxiv a license to display the preprint in perpetuity. It is made available under aCC-BY 4.0 International license.

where τ is a random, exponentially distributed waiting time, until a reaction fires. The probability density function (PDF) for state transition $\mathrm{V} \to \mathrm{T}_1$ can be derived as:

$$\begin{aligned} f_{\mathrm{V}\to\mathrm{T}_1}(x) &= (1 - F_{a_1}(x)) \cdot f_{a_4}(x) \\ &= (1 - (1 - e^{-a_1 x})) \cdot (a_4 e^{-a_4 x}) \\ &= a_4 e^{-(a_1+a_4)x} \end{aligned} \tag{16}$$

where $F_{a_1}(x)$ is the cumulative probability of state transition $\mathrm{V} \to \varnothing$ between time point 0 and x, and $f_{a_4}(x)$ is the probability density function for transition $\mathrm{V} \to \mathrm{T}_1$. In words: The probability that $\mathrm{V} \to \mathrm{T}_1$ occurs and $\mathrm{V} \to \varnothing$ has not occurred yet. Corresponding derivations hold for the process $\mathrm{T}_2 \to \mathrm{T}_2 + \mathrm{V}$:

$$\begin{aligned} f_{\mathrm{T}_2\to\mathrm{T}_2+\mathrm{V}}(x) &= (1 - F_{a_3}(x)) \cdot f_{a_6}(x) \\ &= (1 - (1 - e^{-a_3 x})) \cdot (a_6 e^{-a_6 x}) \\ &= a_6 e^{-(a_3+a_6)x} \end{aligned} \tag{17}$$

For the process $\mathrm{T}_1 \to \mathrm{T}_2$, the probability distribution $f_{a_5}(x)$ is different since the values of a_5 are time-dependent when an integrase inhibitor is applied (as in our example) that affects the reaction according to its pharmacokinetic-pharmacodynamic (PK-PD) properties and its dosing history. Using a Taylor approximation, the probability distribution for $f_{\mathrm{T}_1\to\mathrm{T}_2}(x)$ can be derived as (Supplementary Text S1):

$$f_{\mathrm{T}_1\to\mathrm{T}_2}(x) = (1 - F_{a_2}(x)) \cdot f_{a_5}(x) = a_5(x) e^{-(a_2 x + \int_0^x a_5(t)\, dt)} \tag{18}$$

Method 1: Next Transition Method (NTM)

The precondition for the NTM method is that the concentration-time profile of the prophylactic regimen $\mathcal{S}$ must be known in advance. This can be achieved by solving the deterministic pharmacokinetic equations (7)–(9) for a particular dosing schedule using standard ODE-solvers. Given these pharmacokinetic profiles, the NTM method delivers an extinction probability-time profile. Mathematically, the method calculates $P_E\left(Y_t, \mathcal{S}\right)$.

Now, we can compute $P_E\left(Y_t = \hat{V}, \mathcal{S}\right)$ to denote the extinction probability of unit vector $\hat{V}$, i.e. the probability that a single virus that exists at time t will be cleared in the future. The other two values of interest, which will be outlined further below, are the extinction probability for a T_1 cell and for a T_2 cell, $P_E\left(Y_t = \hat{T_1}, \mathcal{S}\right)$ and $P_E\left(Y_t = \hat{T_2}, \mathcal{S}\right)$, respectively. For brevity, we will skip $\mathcal{S}$ in the notations, keeping in mind that everything refers to a prophylactic strategy with some underlying PK-PD profile that affects reaction rate a_5 in a time-dependent manner.

The extinction probability of one virus at time t, i.e. $P_E\left(Y_t = \hat{V}\right)$, consists of two parts: the probability of direct extinction, with the value $\frac{a_1}{a_1+a_4}$; and the probability that virus is first transformed to T_1, and eventually gets cleared. Since we already know the probability distribution of state transition $\mathrm{V} \to \mathrm{T}_1$, we can split the time into small steps so that the probability of $\mathrm{V} \to \mathrm{T}_1$ can be accurately approximated for each time step. We then get (detailed derivation in Supplementary Text S1):

$$P_E\left(Y_t = \hat{V}\right) = \frac{a_1}{a_1 + a_4} + \sum_{i=1}^{\infty} d_1(t, i) \cdot P_E\left(Y_{t+i\cdot\Delta t} = \hat{T_1}\right) \tag{19}$$

where Δt is a sufficiently small time step and i denotes the number of steps beginning from time point t. The variable $d_1(t, i)$ is a function that represents the probability that

bioRxiv preprint doi: https://doi.org/10.1101/2021.07.22.453374; this version posted July 22, 2021. The copyright holder for this preprint (which was not certified by peer review) is the author/funder, who has granted bioRxiv a license to display the preprint in perpetuity. It is made available under aCC-BY 4.0 International license.

the state transition $\mathrm{V} \to \mathrm{T}_1$ occurs within the ith time step, i.e. $\tau_{\mathrm{V}\to\mathrm{T}_1} \in [t + (i-1)\cdot\Delta t,\, t + i\cdot\Delta t]$ and is given further below.

$P_E\left(Y_t = \hat{T}_2\right)$ is calculated analogously:

$$P_E\left(Y_t = \hat{T}_2\right) = \frac{a_3}{a_3 + a_6} + \sum_{i=1}^{\infty} d_3(t,i) \cdot P_E\left(Y_{t+i\cdot\Delta t} = \hat{T}_2\right) \cdot P_E\left(Y_{t+i\cdot\Delta t} = \hat{V}\right) \quad (20)$$

where $d_3(t,i)$ denotes the probability that the state transition $\mathrm{T}_2 \to \mathrm{V} + \mathrm{T}_2$ occurs within the ith time step. In the equation above, we assumed statistical independence [38], such that $P_E\left(Y_{t+i\cdot\Delta t} = [1,0,1]^T\right) = P_E\left(Y_{t+i\cdot\Delta t} = \hat{T}_2\right) \cdot P_E\left(Y_{t+i\cdot\Delta t} = \hat{V}\right)$.

Since the value of a_5 varies over time, the first term in $P_E\left(Y_t = \hat{T}_1\right)$ is derived in a more general way (Supplementary Text S1):

$$P_E\left(Y_t = \hat{T}_1\right) = \left(1 - \sum_{i=1}^{\infty} d_2(t,i)\right) + \sum_{i=1}^{\infty} d_2(t,i) \cdot P_E\left(Y_{t+i\cdot\Delta t} = \hat{T}_2\right) \quad (21)$$

where the first term is the complement probability of transition $\mathrm{T}_1 \to \mathrm{T}_2$ occurring some time after t.

The probability functions $d_1(t,i)$, $d_2(t,i)$, $d_3(t,i)$ for the respective state transitions can be computed based on eq (16)–(18) as outlined in Supplementary Text S1.

$$\begin{aligned} d_1(t,i) &= -\frac{a_4}{a_1 + a_4} e^{-(a_1+a_4)i\Delta t}\left(1 - e^{(a_1+a_4)\Delta t}\right) \\ d_2(t,i) &= \Delta t \cdot a_5(t + i\cdot\Delta t) \cdot e^{-(a_2\cdot i\cdot\Delta t + \int_t^{t+i\cdot\Delta t} a_5(x)dx)} \\ d_3(t,i) &= -\frac{a_6}{a_3 + a_6} e^{-(a_3+a_6)i\Delta t}\left(1 - e^{(a_3+a_6)\Delta t}\right) \end{aligned} \quad (22)$$

The set of equation for this method is given by eqs (19)–(22). This method is solved iteratively *backwards* using dynamic programming, as exemplified in the pseudocode given in Supplementary Text S2.

This method has foundations in the *embedded Markov Chain*, focusing on all possible one-step state transitions and their corresponding probability. To simulate the time-dependent probabilities of state transition, we performed a time-discretization into sufficiently small steps Δt. Here, we assumed that the extinction probabilities stay approximately unchanged inside each step (we make a zero-order Taylor approximation to compute $d_2(t,i)$), as outlined in the derivation in Supplementary Text S1. Of course, higher-order approximations can also be used. If the time-discretization is omitted altogether, we derive the third method (PGS) as outlined in Supplementary Text S6.

Method 2: Constant Time Step Method (CTSM)

Method 1 can already solve the extinction probability deterministically for a given pharmacokinetic profile, but its computational run time can be further improved. In order to improve the performance, we propose a different set of Ansatz functions to approximate the extinction probability for $\hat{V}, \hat{T}_1$ and $\hat{T}_2$ deterministically.

This method is based on a time-discretization of the underlying time-continuous Markov process into time steps Δt. From the constructed discrete-time Markov chain,

bioRxiv preprint doi: https://doi.org/10.1101/2021.07.22.453374; this version posted July 22, 2021. The copyright holder for this preprint (which was not certified by peer review) is the author/funder, who has granted bioRxiv a license to display the preprint in perpetuity. It is made available under aCC-BY 4.0 International license.

we can compute the extinction probabilities for e.g. state $\hat{V}$ at time point t as follows:

$$\begin{aligned} P_E\left(Y_t = \hat{V}\right) =& P\left(Y_{t+\Delta t} = \mathbf{0} \mid Y_t = \hat{V}\right) + \\ & P\left(Y_{t+\Delta t} = \hat{T_1} \mid Y_t = \hat{V}\right) \cdot P_E\left(Y_{t+\Delta t} = \hat{T_1}\right) + \\ & P\left(Y_{t+\Delta t} = \hat{V} \mid Y_t = \hat{V}\right) \cdot P_E\left(Y_{t+\Delta t} = \hat{V}\right) \end{aligned} \tag{23}$$

with the following interpretations: $P\left(Y_{t+\Delta t} = \mathbf{0} \mid Y_t = \hat{V}\right)$ denotes the probability that the virus is eliminated in time span $[t, t+\Delta t)$; $P\left(Y_{t+\Delta t} = \hat{T_1} \mid Y_t = \hat{V}\right)$ is the probability that the state transition V $\rightarrow$ T_1 occurs in $[t, t+\Delta t)$ and $P_E\left(Y_{t+\Delta t} = \hat{T_1}\right)$ is the probability that a T_1-cell that exists at time $t+\Delta t$ will eventually be eliminated. Finally, the probability that no state transition occurs in $[t, t+\Delta t)$ is given by

$$\begin{aligned} P\left(Y_{t+\Delta t} = \hat{V} \mid Y_t = \hat{V}\right) = 1 &- P\left(Y_{t+\Delta t} = \mathbf{0} \mid Y_t = \hat{V}\right) \\ &- P\left(Y_{t+\Delta t} = \hat{T_1} \mid Y_t = \hat{V}\right). \end{aligned}$$

The terms $P\left(Y_{t+\Delta t} = \mathbf{0} \mid Y_t = \hat{V}\right)$ and $P\left(Y_{t+\Delta t} = \hat{T_1} \mid Y_t = \hat{V}\right)$ can be derived based on the calculations for the distribution of state transition events, as outlined in Supplementary Text S1. Using these derivations, the the final expression for $P_E\left(Y_t = \hat{V}\right)$ is

$$\begin{aligned} P_E\left(Y_t = \hat{V}\right) =& \frac{a_1}{a_1 + a_4}\left(1 - e^{-(a_1+a_4)\Delta t}\right) \\ &+ \frac{a_4}{a_1 + a_4}\left(1 - e^{-(a_1+a_4)\Delta t}\right) \cdot P_E\left(Y_{t+\Delta t} = \hat{T_1}\right) \\ &+ e^{-(a_1+a_4)\Delta t} \cdot P_E\left(Y_{t+\Delta t} = \hat{V}\right) \end{aligned} \tag{24}$$

Similarly, for $P_E\left(Y_t = \hat{T_1}\right)$ we get:

$$\begin{aligned} P_E\left(Y_t = \hat{T_1}\right) =& \frac{a_2}{a_2 + a_5(t)}\left(1 - e^{-(a_2+a_5(t))\Delta t}\right) \\ &+ \frac{a_5(t)}{a_2 + a_5(t)}\left(1 - e^{-(a_2+a_5(t))\Delta t}\right) \cdot P_E\left(Y_{t+\Delta t} = \hat{T_2}\right) \\ &+ e^{-(a_2+a_5(t))\Delta t} \cdot P_E\left(Y_{t+\Delta t} = \hat{T_1}\right) \end{aligned} \tag{25}$$

and for $P_E\left(Y_t = \hat{T_2}\right)$:

$$\begin{aligned} P_E\left(Y_t = \hat{T_2}\right) =& \frac{a_3}{a_3 + a_6}\left(1 - e^{-(a_3+a_6)\Delta t}\right) \\ &+ \frac{a_6}{a_3 + a_6}\left(1 - e^{-(a_3+a_6)\Delta t}\right) \cdot P_E\left(Y_{t+\Delta t} = \hat{T_2}\right) \\ &\cdot P_E\left(Y_{t+\Delta t} = \hat{V}\right) + e^{-(a_3+a_6)\Delta t} \cdot P_E\left(Y_{t+\Delta t} = \hat{T_2}\right) \end{aligned} \tag{26}$$

Similar to the next transition method (NTM), when implementing the constant time step method, we make a zero-order Taylor approximation to $a_5(s)$ as visible in eq (25) and assumed that all extinction probabilities P_E stay unchanged for each time step $s \in [t, t+\Delta t)$. The implementation for this method is outlined in the pseudo-code in Supplementary Text S3. Similar to the previous method, the CTSM is solved iteratively *backwards* in time using dynamic programming.

bioRxiv preprint doi: https://doi.org/10.1101/2021.07.22.453374; this version posted July 22, 2021. The copyright holder for this preprint (which was not certified by peer review) is the author/funder, who has granted bioRxiv a license to display the preprint in perpetuity. It is made available under aCC-BY 4.0 International license.

Method 3: Probability Generating System (PGS)

In the CTSM, we constructed a discrete-time Markov Chain for time steps Δt and approximated $a_5(s)$ within such a time-step $s \in [t, t+\Delta t)$ using a zero-order Taylor approximation, i.e. $a_5(s) \approx a_5(t)$. Because of this approximation, the precision of the method depends on Δt. On the contrary, for the PGS we will take $\Delta t \to 0$ to derive a set of continuous Ansatz functions. With this idea in mind, we differentiate eqs. (24)–(26) to derive the following set of ordinary differential equations (Supplementary Text S1):

$$\begin{aligned}
\frac{dP_E\left(Y_t = \hat{V}\right)}{dt} &= a_1 \cdot \left(P_E\left(Y_t = \hat{V}\right) - 1\right) \\
&\quad + a_4 \cdot \left(P_E\left(Y_t = \hat{V}\right) - P_E\left(Y_t = \hat{T}_1\right)\right) \\
\frac{dP_E\left(Y_t = \hat{T}_1\right)}{dt} &= a_2 \cdot \left(P_E\left(Y_t = \hat{T}_1\right) - 1\right) \\
&\quad + a_5(t) \cdot \left(P_E\left(Y_t = \hat{T}_1\right) - P_E\left(Y_t = \hat{T}_2\right)\right) \\
\frac{dP_E\left(Y_t = \hat{T}_2\right)}{dt} &= a_3 \cdot \left(P_E\left(Y_t = \hat{T}_2\right) - 1\right) + a_6 \cdot \left(P_E\left(Y_t = \hat{T}_2\right)\right. \\
&\quad \left. - P_E\left(Y_t = \hat{T}_2\right) \cdot P_E\left(Y_t = \hat{V}\right)\right)
\end{aligned} \tag{27}$$

Given $a_5(t)$ and initial values, equations above can be solved by any ODE solver, as outlined in in Supplementary Text S4.

Implementation and availability

Pseudocodes for the three methods are described in detail in Supplementary Texts S2–4. All methods were implemented in Python 3.8, using SciPy 1.5.0, Numpy 1.18.5, Pandas 1.0.5 and matplotlib 3.2.2. Codes are available from `https://github.com/KleistLab/PrEP.git`.

Algorithmic specifications

Next transition method (NTM). For NTM, we chose a time step of $\Delta t = 1$ min. Furthermore, the method requires look-ahead horizons $k_1, \ldots, k_3$ which are automatically determined for a given precision parameter ξ (Supplementary Text S2). Throughout the manuscript we use $\xi = 0.999$.

In this work, we extended the end time point for an extra $\tau = 100 hours$ so that the values in the target time interval are accurate. This value of extra time can be determined roughly from the half life of considered drugs, e.g $\tau \approx 7 \cdot t_{1/2}$, where $t_{1/2} \approx 14.5 hours$ denotes the half life of DTG. The above stated criterium guarantees that the drug concentrations at $T_e + \tau$ are $< 1\%$ of the trough concentrations. Lastly, the method is solved backwards from an end time $T_e + \tau$ to some start time T_s. At $T_e + \tau$, we initialize the extinction probabilities with the values in the absence of drugs, e.g. $P_E(Y_{T_e} = \hat{V}, \mathcal{S}) = P_E(\hat{V}, \varnothing), P_E(Y_{T_e} = \hat{\mathrm{T}}_1, \mathcal{S}) = P_E(\hat{\mathrm{T}}_1, \varnothing)$ and $P_E(Y_{T_e} = \hat{\mathrm{T}}_2, \mathcal{S}) = P_E(\hat{\mathrm{T}}_2, \varnothing)$, which can be determined analytically [38].

Constant time step method (CTSM). For CTSM, we set $\Delta t = 1$ min. Noteworthy, the simulation time horizon must exceed the time horizon of interest to ensure that the drug concentration is approaching 0. This is done as explained for the NTM. We then initialize the extinction probabilities with the values in the absence of drugs before solving the set of equations *backwards* in time.

bioRxiv preprint doi: https://doi.org/10.1101/2021.07.22.453374; this version posted July 22, 2021. The copyright holder for this preprint (which was not certified by peer review) is the author/funder, who has granted bioRxiv a license to display the preprint in perpetuity. It is made available under aCC-BY 4.0 International license.

Probability generating system (PGS). The PGS does not require to pre-define a time-step (this is done by the ODE solver). Like with the other methods, the simulation time horizon is extended analogously and the extinction probabilities are initiated with the values in the absence of drugs. We use `solve_ivp` in `SciPy` [40] with the LSODA solver (linear multistep method) and default settings to solve the system of ODEs *backwards* in time.

EXTRANDE. We implemented the exact stochastic simulation method EXTRANDE with configurations identical to [11].

Pharmacokinetics. Pharmacokinetic profiles for DTG were pre-computed from eqs (7)–(9) using `solve_ivp` in `SciPy` [40] with default solver and default settings, for the respective prophylactic regimens $\mathcal{S}$. Depending on the algorithm, D_t was either evaluated at discrete time points $t = i \cdot \Delta t$ (NTM, CTSM), or linearly interpolated (PGS, EXTRANDE). Using the pharmacokinetic profiles, the time-dependent value of $\eta_D(t)$, eq (11) was determined and used in the respective algorithms. Depending on the analysis, we either simulated DTG pharmacokinetics for a representative individual, or by drawing pharmacokinetic parameters for 1000 virtual individuals from the parameter distributions defined in [11].

Simulation of pre- and post-exposure prophylaxis

Single viral challenge. For single viral challenges the profiles of $P_E(Y_t = \hat{V}, \mathcal{S}), P_E(Y_t = \hat{\mathrm{T}}_1, \mathcal{S})$ and $P_E(Y_t = \hat{\mathrm{T}}_2, \mathcal{S})$ were computed using NTM, CTSM and PGS with configurations outlined above.

Multiple viral challenges. Using the new methods, we can also compute the prophylactic efficacy following multiple viral challenges: Under the assumption of statistical independence [38], the extinction probability following multiple viral challenges is the product of extinction probabilities for single viral challenges at their corresponding time points. I.e.:,

$$\varphi(Y_{\{t_i\}}, \mathcal{S}) = 1 - \frac{P_I(Y_{\{t_i\}}, \mathcal{S})}{P_I(Y_{\{t_i\}}, \varnothing)}. \tag{28}$$

with $\{t_i\}$, $i = 1, \ldots, n$ denotes a set of n viral exposures and

$$P_I(Y_{\{t_i\}}) = 1 - \prod_i P_E(Y_{t_i})$$

due to statistical independence, where $P_E(Y_{t_i})$ is computed as described above.

If n viral exposures occur at the same time $t_i = t$, we have

$$P_I(Y_{\{t_i\}}) = 1 - \big(P_E(Y_t)\big)^n.$$

To assess the validity of this assumption we also simulated multiple viral challenges with EXTRANDE and compared the results.

Computation of density function of the extinction event

So far, we computed the probability that viral extinction is eventually happening after viral exposure at some time t; $P_E\left(Y_t = \hat{V}, \mathcal{S}\right)$. I.e., we only care if extinction eventually occurs, regardless of *when* it happens.

The introduced methods can however also be used to estimate the probability that the extinction occurs in a specific time range. To solve for this probability, we can e.g. alter the initial conditions of the PGS. In essence, we are interested in the extinction probability within a time range $[t_0, t_e]$. Since equations (27) are solved backwards in

bioRxiv preprint doi: https://doi.org/10.1101/2021.07.22.453374; this version posted July 22, 2021. The copyright holder for this preprint (which was not certified by peer review) is the author/funder, who has granted bioRxiv a license to display the preprint in perpetuity. It is made available under aCC-BY 4.0 International license.

time (Supplementary Text S4), we initialize the set of ODEs with the probability that the extinction occurs at the final time point t_e, for example $P\left(Y_{t_e} = \mathbf{0} \mid Y_{t_e} = \hat{V}\right)$ for the first ODE (eq. (27)). This probability is obviously 0. Consequently, the set of ODEs eq. (27) is initialized with values $[0, 0, 0]$ and then solved backwards in time until t_0. The derived probabilities have the following interpretation: they denote the probability that a single virus, single T_1 and single T_2, transmitted at time point t_0 are cleared in the time range $[t_0, t_e]$. For example, if we want to determine the probability that virus is cleared $t_e = 10$ days after exposure to one infectious virus (at day t_0) for some prophylactic regimen, we set the time span of the ODE set eq. (27) to $[0, 10]$, initialize the ODE with $[0, 0, 0]^T$ at $t_e = 10$ and solve the PGS backwards to $t_0 = 0$ to derive $P\left(Y_{t_e} = \mathbf{0}, \mathcal{S} \mid Y_{t_0} = \hat{V}\right)$ in the first equation of the PGS, eq. (27). For a given pharmacokinetic (PK) profile D_t this process has to be repeated for different values of t_e to reconstruct the entire cumulative probability density function (CDF) with the correct PK profile. The probability density function (PDF) can be derived straight-forward from the CDF. Similarly, the procedure also allows to compute the corresponding probabilities for arbitrary numbers of initial viruses (statistical independence assumption), eq. (14).

Results

Efficacy of PrEP-on-demand with DTG

Using the three proposed methods, we computed the time course of the extinction probability $P_E(Y_t, \mathcal{S})$ and the corresponding prophylactic efficacy $\varphi(Y_t, \mathcal{S})$ for a 3-days once daily short-course oral 50mg DTG prophylaxis, that was either initiated shortly after viral exposure (post-exposure prophylaxis, PEP) or before virus exposure (pre-exposure prophylaxis, PrEP). Fig. 2A shows the profiles of the extinction probability and Fig. 2B depicts the corresponding prophylactic efficacy. In Figure 2, for illustration, we depict these quantities for $Y_t = \hat{V}, Y_t = \hat{T}_1$ and $Y_t = \hat{T}_2$ individually. From these quantities, the extinction probability for an arbitrary initial state can be calculated based on eq (14). All three proposed methods yielded indistinguishable results. In the figure we therefore only display the results of the PGS.

From a computational point of view, PEP and PrEP are computed within the same execution of the proposed methods: A pharmacokinetic trajectory (brown dashed line in Fig. 2A & B) is placed on the time axis and the methods are backwards propagated to some time before the first dose of the drug was given. Any time points *before* the first dose denote PEP, whereas PrEP refers to time points *after* the first dose of the drug. For example, the value of the red line in Fig. 2B at $t = -2$ (days) indicates that the efficacy of a 3 days 50mg oral DTG post-exposure prophylaxis, that was initiated 2 days after exposure to a single virus particle, is about 35%. If exposure occurred at $t = 0$ (coinciding with the first drug intake), the efficacy would be $\approx 90\%$. As described above, the new methods therefore compute a prophylactic efficacy profile for a time span of interest, i.e. every point on this time-efficacy curve represents the prophylactic efficacy $\varphi(Y_t, \mathcal{S}_{t_0})$ conditioned that the viral exposure occurred at the indicated time point and the prophylactic regimen $\mathcal{S}$ was started at $t_0 = 0$.

From a biological point of view, Figure 2B nicely highlights the role of the molecular target of the integrase inhibitor DTG within the viral replication cycle [38]: The drug is able to potently prevent infection if it emanates from a virus V or a T_1 cell (compartments *proceeding* its molecular target process), but not from a T_2 (a compartment *succeeding* its molecular target process).

While the three proposed methods yielded indistinguishable results for the presented

bioRxiv preprint doi: https://doi.org/10.1101/2021.07.22.453374; this version posted July 22, 2021. The copyright holder for this preprint (which was not certified by peer review) is the author/funder, who has granted bioRxiv a license to display the preprint in perpetuity. It is made available under aCC-BY 4.0 International license.

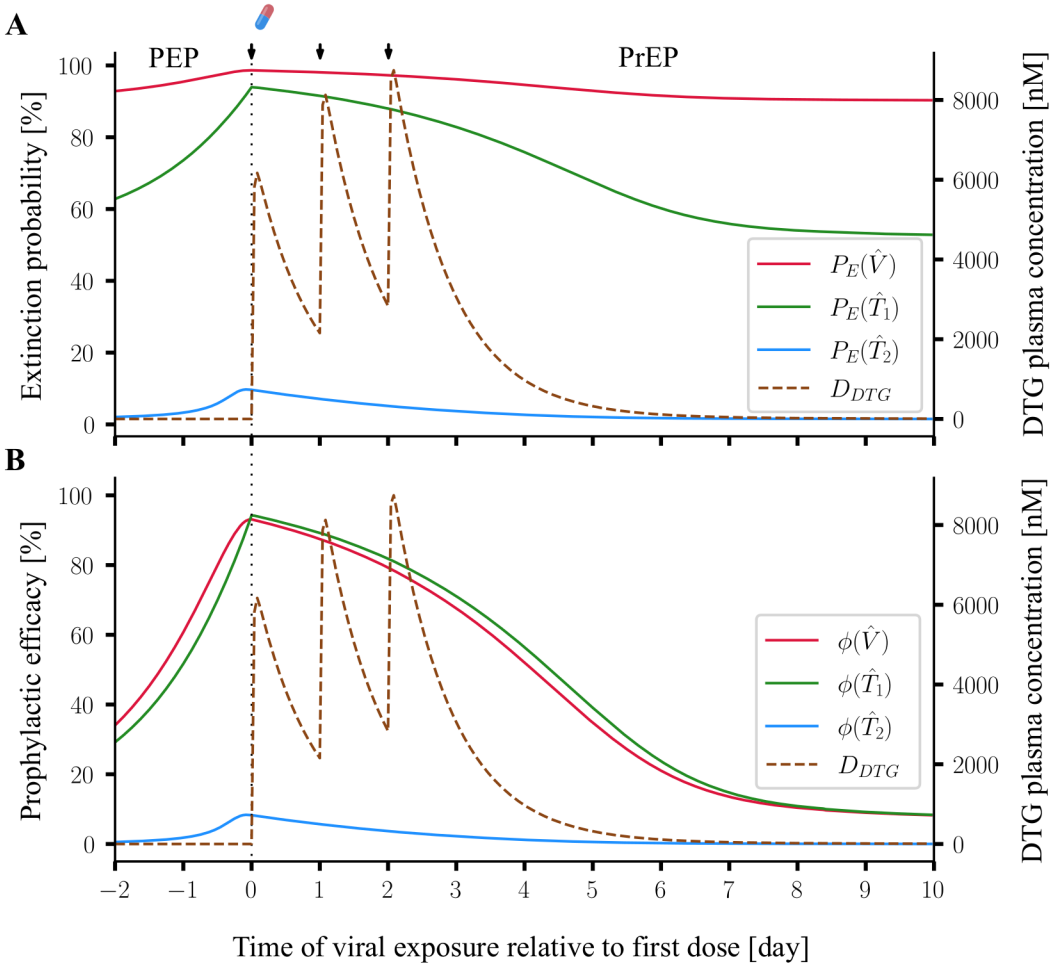

Fig 2. Prophylactic efficacy for 3-days once daily short-course oral 50mg DTG. The extinction probabilities were computed by PGS, for a representative individual with pharmacokinetic parameters $k_a = 2.24\text{h}^{-1}$, $V_p/F_{bio} = 0.73$ L, $Q/F_{bio} = 0.0082$ L/h, $CL/F_{bio} = 0.85$ L/h and $V_c/F_{bio} = 17.7$ L. Observation began from two days before the first dose (the drug-doses are marked by arrows), until the 10th day after the first dose of DTG. The X-axis denotes the timing of viral exposure relative to the first dose, i.e. negative values represent a viral exposure before the first dose of DTG (post-exposure prophylaxis, PEP), whereas positive values represent pre-exposure prophylaxis (PrEP) scenarios. **A:** DTG plasma concentration (dashed brown line) and the extinction probability profiles, with regards to one virus $P_E(\hat{V}, \mathcal{S})$, one T_1-cell $P_E(\hat{T}_1, \mathcal{S})$ and one T_2-cell $P_E(\hat{T}_2, \mathcal{S})$ are shown by solid red, green and blue lines. **B:** DTG plasma concentration (dashed brown line) and the corresponding prophylactic efficacies for one virus $\varphi(\hat{V}, \mathcal{S})$, one T_1-cell $\varphi(\hat{T}_1, \mathcal{S})$ and one T_2-cell $\varphi(\hat{T}_2, \mathcal{S})$ are shown by solid red, green and blue lines.

example (Fig. 2), their run times were markedly different, Table 2: While NTM required about three minutes on a AMD R5 core with 3.6 Ghz and 16 GB RAM, CTSM only needed 5.9 seconds and PGS ran in a fraction of a second. Notably, if stochastic simulation was performed (as in [11]), several thousand stochastic samples need to be

bioRxiv preprint doi: https://doi.org/10.1101/2021.07.22.453374; this version posted July 22, 2021. The copyright holder for this preprint (which was not certified by peer review) is the author/funder, who has granted bioRxiv a license to display the preprint in perpetuity. It is made available under aCC-BY 4.0 International license.

generated to approximate the prophylactic efficacy $\varphi(Y_t, \mathcal{S})$ from the sample statistic for a single time point t.

Table 2. Run time of the proposed methods.

Method	run time $[s]$
NTM	185.14
CTSM	5.88
PGS	0.21

Run time to compute the prophylactic profiles in Fig. 2 on an single AMD R5 core with 3.6 Ghz and 16 GB RAM.

Comparison with stochastic simulation (EXTRANDE)

Previously, an exact hybrid stochastic simulation method called EXTRANDE was introduced in [41]. We subsequently adapted the algorithm to estimate PrEP efficacy against HIV [11, 12]. Here, we used EXTRANDE to verify the accuracy of the proposed methods. Fig. 3 shows the predicted efficacy of a three days prophylaxis with either 2 or 50mg oral DTG started at $t = 0$ using EXTRANDE vs. the proposed methods. In contrast to Fig. 2 (drug-centered evaluation), here we perform an exposure-centered evaluation to calculate $\varphi(Y_{t_0} = \hat{V}, \mathcal{S}_{t_i})$. I.e. the virus exposure occurs $t_0 = 0$ and the first dose is taken at time $t_i \in \{-23, -18, -12, -6, -3, -1, 2, 4, 6, 12, 18, 24\}$ hours before/past the viral exposure. In words: the prophylactic efficacy if exposure to a single virus particle occurred at time $t_0 = 0$ and the 3-day prophylaxis was initiated at time t_i.

In Fig. 3, we can see that the three proposed methods yield highly similar results (overlapping green, blue and orange lines) and moreover that the results of the proposed methods form smooth lines. The results of EXTRANDE fluctuate randomly around the results of the proposed methods. From a biological standpoint we see that the prophylactic efficacy 50mg DTG is almost double compared to 2mg. Moreover, we see that the prophylactic efficacy deteriorates much faster for PEP than for PrEP. I.e., if DTG is taken as PEP, it needs to be taken shortly after the exposure. For PrEP-on demand, the efficacy changes only marginally if PrEP is initiated within 24 hours prior to exposure.

In terms of run time, EXTRANDE requires thousands of simulations to achieve statistically reliable meaningful results. In Fig 3, for each of the 12 time points we ran 10 000 simulations with EXTRANDE, which took about two hours for all points using multi-treading (12 treads). By contrast, using the proposed methods, the values of all time points can be extracted from a single run, i.e. $\varphi(Y_{t_0} = \hat{V}, \mathcal{S}_{t_i}) = \varphi(Y_{-t_i} = \hat{V}, \mathcal{S}_{t_0})$, with run times depicted in (Table 2).

Obviously, the pharmacokinetic profiles can be arbitrarily altered, which allows to assess the prophylactic efficacy of any regimen $\mathcal{S}$, e.g. with regards to the drugs taken, their dose, the administration frequency and the timing of drug intake, as outlined above.

PrEP efficacy for multiple viral challenges and different inoculum sizes

Another interesting application of the proposed methods is to assess the impact of the exposure on the prophylactic efficacy, e.g. to assess the sensitivity of $\varphi(Y_t, \mathcal{S}_{t_0})$ with regards to Y_t. We have shown previously by simulations [23] that the prophylactic efficacy depends on the inoculum size (= how many viruses enter a replication-enabling

bioRxiv preprint doi: https://doi.org/10.1101/2021.07.22.453374; this version posted July 22, 2021. The copyright holder for this preprint (which was not certified by peer review) is the author/funder, who has granted bioRxiv a license to display the preprint in perpetuity. It is made available under aCC-BY 4.0 International license.

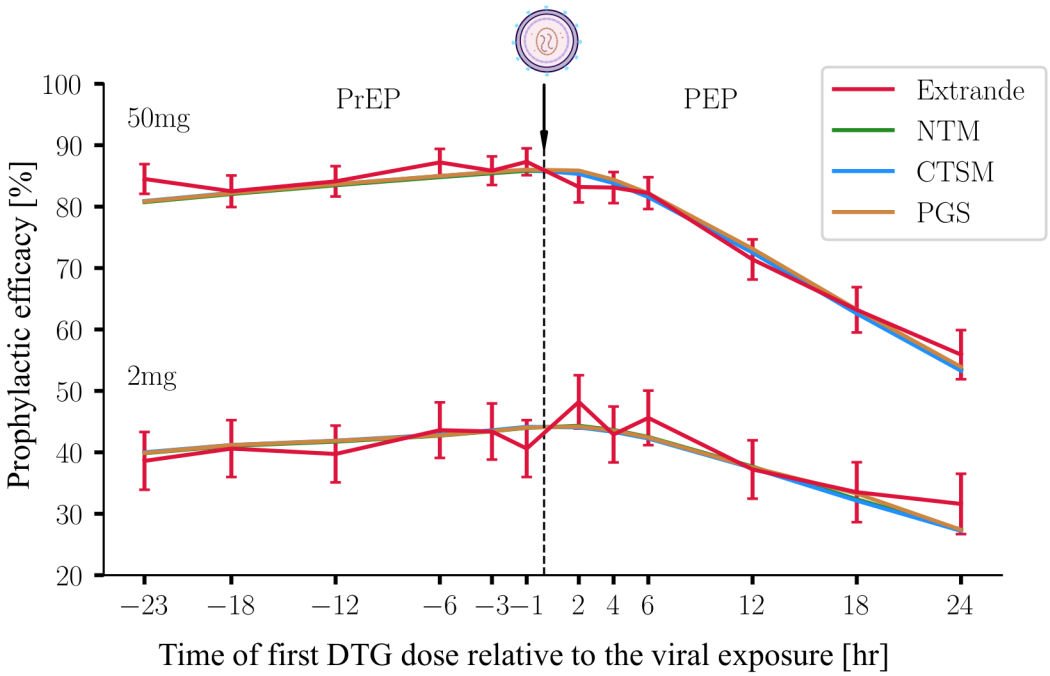

Fig 3. Prophylactic efficacy for PrEP and PEP computed by EXTRANDE and the new methods. 2 mg (lines below) and 50 mg (lines above) DTG were ingested for three days, respectively. The extinction probabilities were computed by EXTRANDE and the three new methods, for a representative individual with pharmacokinetic parameters $k_a = 2.24\text{h}^{-1}$, $V_p/F_{bio} = 0.73$ L, $Q/F_{bio} = 0.0082$ L/h, $CL/F_{bio} = 0.85$ L/h and $V_c/F_{bio} = 17.7$ L. The prophylactic efficacy was computed using eq. (12) for initial state $Y_0 = [1, 0, 0]^T$. The X-axis represents the timing of the first DTG dose relative to the virus challenge, which is marked by the arrow. EXTRANDE was run 10 000 times for each condition. The error bars denote the 95% confidence bounds for the ensemble estimate, computed using the Greenwood's formula [42].

environment). Also, in [24], we used stochastic simulation to assess prophylactic efficacy after multiple viral challenges. Here, we demonstrate how the proposed method can be used to address these questions.

Multiple Challenges. Multiple viral challenges can be computed straight-forward as exemplified in the *Methods* section. In Table 3 we show the estimated prophylactic efficacy for different PrEP regimen (either 3 or 7 doses of 2 or 50mg DTG started at $t_0 = 0$) with multiple challenges to a single virus particle, computed using both PGS and EXTRANDE. Foremost, as a sanity check, we can see that both methods yield congruent results for all tested conditions. We can also see that higher dose, as well as a longer time course (seven vs. three days) of DTG dosing improves the prophylactic efficacy, even if more viral challenges occur during the short-course prophylaxis. Also, we observe a interesting interplay between the number of exposures and their timing: For example, if two exposures occur at 1 and 24h after the first dose of DTG vs. three exposures at 1, 24 and 72h after DTG initiation, we see a decrease in efficacy. However, when we compare two exposures occur at 1 and 72h after the first dose of DTG vs. three exposures at 1, 24 and 72h after DTG initiation, we see a slight increase in efficacy. This has the following reason: In the presented example, the prophylactic

bioRxiv preprint doi: https://doi.org/10.1101/2021.07.22.453374; this version posted July 22, 2021. The copyright holder for this preprint (which was not certified by peer review) is the author/funder, who has granted bioRxiv a license to display the preprint in perpetuity. It is made available under aCC-BY 4.0 International license.

efficacy (relative risk) after multiple challenges is given by:

$$\varphi(Y_{\{t_i\}}, \mathcal{S}) = 1 - \frac{P_I(Y_{\{t_i\}}, \mathcal{S})}{P_I(Y_{\{t_i\}}, \varnothing)}. \tag{29}$$

where $\{t_i\}$, $i = 1, \ldots, n$ denotes a set of n viral exposures.

Table 3. Prophylactic efficacy in case of multiple viral challenges.

Dose	# Doses	Exposure time	Prophylactic efficacy [%]		Probability of Infection [%]	
			EXTRANDE	PGS	$P_I(Y_{\{t_i\}}, \mathcal{S})$	$P_I(Y_{\{t_i\}}, \varnothing)$
2mg	3	1, 24h	39.64 ± 1.05	40.52	11.11	18.68
	3	1, 72h	27.72 ± 1.13	27.02	13.63	18.68
	3	1, 24, 72h	29.90 ± 0.91	29.64	18.76	26.67
	7	1, 24, 72, 144h	44.31 ± 0.73	44.92	18.66	33.87
50mg	3	1, 24h	82.71 ± 0.59	82.58	3.25	18.68
	3	1, 72h	72.21 ± 0.74	72.27	5.18	18.68
	3	1, 24, 72h	73.33 ± 0.60	73.79	6.99	26.67
	7	1, 24, 72, 144h	87.31 ± 0.37	87.25	4.31	33.87

2 or 50mg oral DTG was ingested for 3 and 7 days respectively starting at $t_0 = 0$, and 2–4 viral exposures occurred at the time 'Exposure time' hours after DTG initiation. During each exposure one infectious virus entered a replication-enabling compartment. The corresponding prophylactic efficacy was computed by PGS and EXTRANDE, respectively. For each condition EXTRANDE was run 100 000 times. The 95% confidence bounds of the EXTRANDE estimate was computed using the Greenwoods formula [42]. The probability of infection after multiple viral challenges with- and without drug ($P_I(Y_{\{t_i\}}, \mathcal{S})$ and $P_I(Y_{\{t_i\}}, \varnothing)$) were computed with PGS and are depicted in the last 2 columns. Utilized pharmacokinetic parameters were $k_a = 2.24\text{h}^{-1}$, $V_p/F_{bio} = 0.73$ L, $Q/F_{bio} = 0.0082$ L/h, $CL/F_{bio} = 0.85$ L/h and $V_c/F_{bio} = 17.7$ L.

Now, if $P_I(Y_{\{t_i\}}, \varnothing)$ increases faster with the number of exposures than $P_I(Y_{\{t_i\}}, \mathcal{S})$, a scenario may arise, in which the prophylactic efficacy (= relative risk reduction) may be higher, although more exposures happened. I.e. the contextual information, '*when did the exposure(s) occur relative to the drug dosing*' is relevant. For example, if many exposures happened at times of almost full protection, the exposed person would be better off than if only a few exposures happened at times of low protection.

Inoculum size. Fig. 4 shows how the profile of prophylactic efficacy is affected by the number of inoculated viruses. This can be calculated from the solution of the PGS is a straight forward way, akin to eq. (14) (statistical independence assumption). In Fig. 4, we observe that different inculum sizes lead to an (exponential) scaling of the prophylactic efficacy, and that the efficacy deteriorates, when large numbers of viruses are able to reach a replication-competent compartment.

Long-term prophylactic efficacy

Because of its superior computational performance, the PGS can also be applied to estimate prophylactic efficacy over very long time scales for population pharmacokinetics (Pop-PK). I.e., typically pharmacokinetic variability is described by statistical models, such as non-linear mixed effects models (NLME), e.g. in [11]. If the pharmacokinetic characteristics of an individual are not known, a Pop-PK model may still be used to accurately capture likely pharmacokinetic profiles in an individual, given a dosing history. The PGS would then allow to predict the profile of prophylactic protection if the individual was exposed to virus at any time during the observation horizon. Note that this type of analysis is usually not feasible with stochastic methods, due to computational demands (for each time point in the profile, several thousand stochastic simulations would be required).

bioRxiv preprint doi: https://doi.org/10.1101/2021.07.22.453374; this version posted July 22, 2021. The copyright holder for this preprint (which was not certified by peer review) is the author/funder, who has granted bioRxiv a license to display the preprint in perpetuity. It is made available under aCC-BY 4.0 International license.

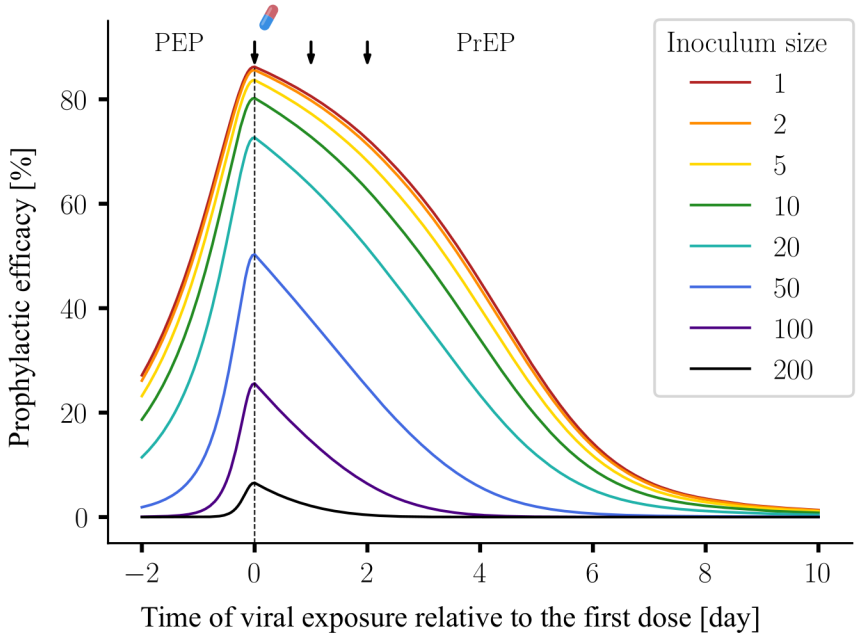

Fig 4. Profiles of prophylactic efficacy for different inoculum sizes. The experimental setup was chosen identical to Fig 2. To calculate the prophylactic efficacy profiles, an exponential scaling is applied to the solutions of the PGS (eq (14)). The solutions are plugged into eq (12).

In Fig. 5, we show the estimated long-term efficacy profile for a chronic, 6-month once-daily 50mg oral DTG regimen for different levels of adherence. For each adherence level the computation was conducted on 1000 virtual individuals sampled from the Pop-PK model to capture inter-individual differences in drug pharmacokinetics. The red line and the grey ranges denote the median, interquartile and $2.5\% - 97.5\%$ ranges of prophylactic efficacy under consideration of inter-individual differences in the pharmacokinetic profiles. With PGS it took about 24 min in total to compute the 6-month prophylactic profiles for 1000 virtual individuals and a given sequence of dosing events (determined by the adherence level), i.e. less than 1.5s for each individual on an AMD R5 core with 3.6Ghz and 16GB RAM (standard laptop). This computation could also be easily parallelized, which would reduce the run time considerably (the entire simulation took about 5 min on the same computer with 12 threads).

Density function of the extinction event

Using the approaches outlined in the *Methods* section, it is also possible to compute *when* the actual extinction event happens after exposure. This is highly useful in determining how long a prophylaxis on-demand should be given.

Fig. 6 shows the cumulative probability of extinction, as well as the density function of the extinction event, computed using the PGS for a 3days 50mg DTG regimen that was initiated at $t_0 = 0$, coinciding with viral exposure. In these simulations, akin to the last example, we sample virtual individuals from the Pop-PK model.

Fig 6A and B depict the cumulative-, as well as the density function of the extinction event after exposure to a single initial virus. Fig 6C and D show the corresponding distributions after exposure to 20 viruses. From the figures, we can see

bioRxiv preprint doi: https://doi.org/10.1101/2021.07.22.453374; this version posted July 22, 2021. The copyright holder for this preprint (which was not certified by peer review) is the author/funder, who has granted bioRxiv a license to display the preprint in perpetuity. It is made available under aCC-BY 4.0 International license.

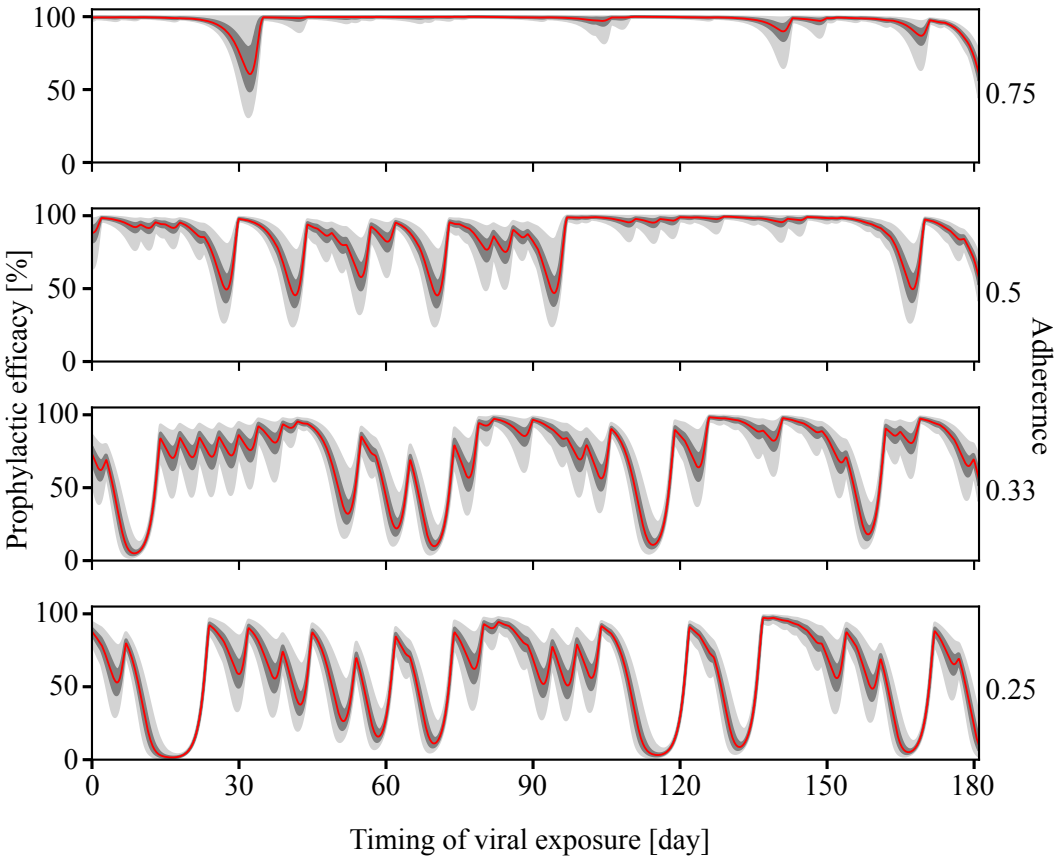

Fig 5. Long-term prophylactic profile with different levels of adherence. $N = 1000$ virtual patients were sampled from the pharmacokinetic parameter distributions defined in Table 2 of [11]. 50 mg dose of DTG / day was ingested in this six-month-long regimen with adherence level of 0.75, 0.5, 0.33 and 0.25. The red line depicts the median predicted prophylactic efficacy, whereas the dark- and light grey areas present the quartile range and the $2.5\% - 97.5\%$ range respectively. The prophylactic efficacy was computed for $Y_0 = [1, 0, 0]^T$.

that the cumulative probability of viral extinction is much lower after exposure to 20- compared to one virus (panel A vs. C). Moreover, we can see that, after exposure to a single virus, extinction most likely occurs shortly after exposure, e.g. within 1–2 days. In contrast, when 20 viruses are inoculated, extinction is most likely happening at day 4 after exposure, and that it is still likely that extinction may occur up to 10 days after exposure when a 3days 50mg DTG prophylaxis is applied. Moreover, extinction is less likely to happen: After exposure to 20 viruses, extinction occurs in 10 days with about 75% probability (median), compared to 98% after exposure to a single virus.

In other words, our modelling highlights that the prophylactic efficacy depends on the magnitude of exposure. Moreover, the duration to eliminate the virus is prolonged when more virus becomes inoculated. Essentially, this suggests that large inocula, which may occur after blood transfusions, needle stick exposures, or tissue rupture during sexual contact may require longer duration of prophylaxis to prevent infection.

bioRxiv preprint doi: https://doi.org/10.1101/2021.07.22.453374; this version posted July 22, 2021. The copyright holder for this preprint (which was not certified by peer review) is the author/funder, who has granted bioRxiv a license to display the preprint in perpetuity. It is made available under aCC-BY 4.0 International license.

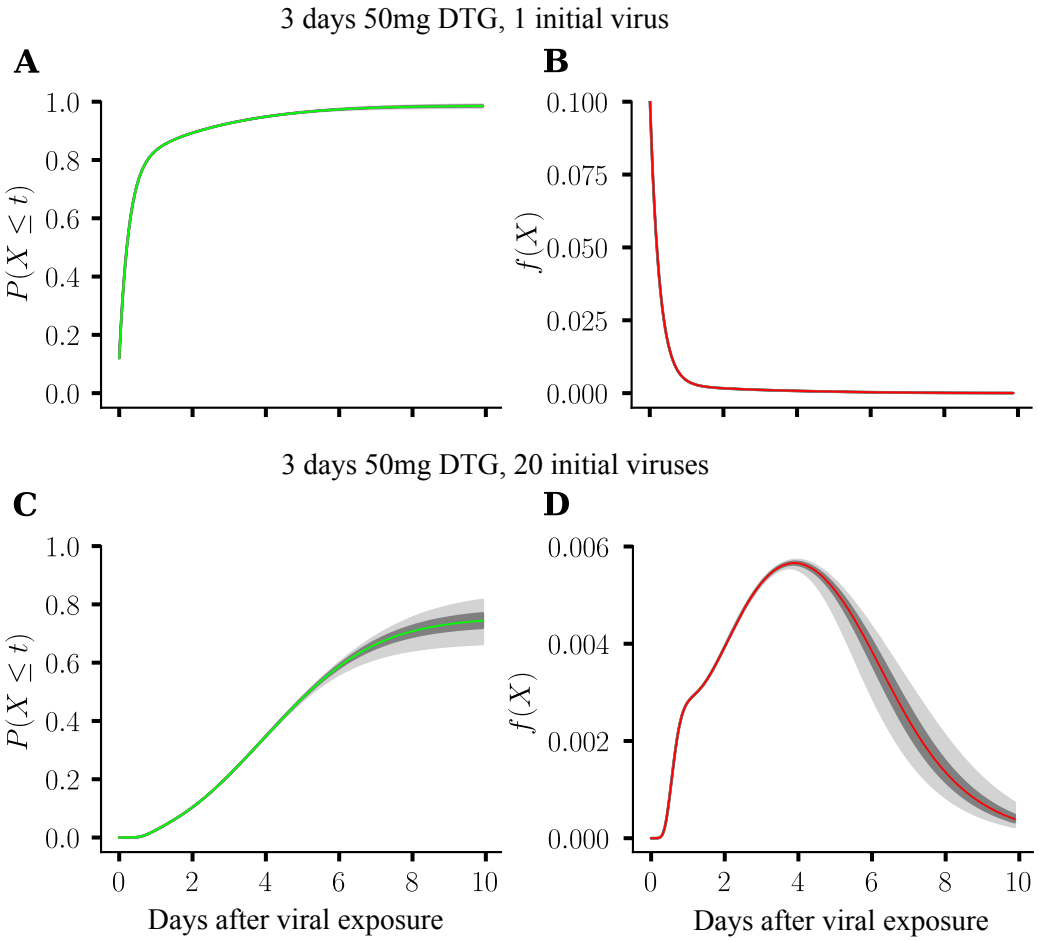

Fig 6. Cumulative probability and probability density function of extinction event. $N = 1000$ virtual patients were sampled from the pharmacokinetic parameter distributions defined in Table 2 of [11]. 50 mg dose of DTG / day was ingested for three days, first dose was taken at $t_0 = 0$, coinciding with viral exposure. A: cumulative extinction probability for one initial virus. B: probability density function of extinction for one initial virus. C: cumulative extinction probability for 20 initial viruses. D: probability density function of extinction for 20 initial viruses. The red and green lines depict the respective median values, whereas the dark- and light grey areas present the quartile range and $2.5\% - 97.5\%$ confidence range, taking inter-individual pharmacokinetic differences into account.

Discussion

The prophylactic efficacy of novel drug candidates against HIV is determined by the complex interplay of enzymatic, cellular, viral, immunological, pharmacological, as well as behavioural factors [18]. Some of these factors can be described in experimental surrogate systems [43]. However, their complex interplay, which determines clinical efficacy, can usually not be fully described using *in vitro* or *ex vivo* experiments. Moreover, animal models for HIV prophylaxis are suitable for proof-of-concept studies, but may still be confounded by inter-species differences, as well as differences in the viruses used [44]. Lastly, while clinical studies of HIV prophylaxis are useful to assess

bioRxiv preprint doi: https://doi.org/10.1101/2021.07.22.453374; this version posted July 22, 2021. The copyright holder for this preprint (which was not certified by peer review) is the author/funder, who has granted bioRxiv a license to display the preprint in perpetuity. It is made available under aCC-BY 4.0 International license.

the relevant efficacy endpoint, they do not allow to disentangle the complex interplay between the aforementioned factors, because of inherent limitations in the study design, sample sizes and the inability to measure the joint interplay of parameters that determine clinical efficacy. Therefore, it remains a formidable challenge to identify factors that alter prophylactic efficacy, or parameters that can be improved by the development of novel drugs or drug formulations for HIV prophylaxis.

Mathematical models [11, 12, 21–24, 28, 45–47] have become an essential tool to complement our knowledge about prophylactic efficacy of antiviral compounds, as they are able to put the different parameters in context and test their relevance for determining prophylactic efficacy. Stochastic simulation methods are currently the gold standard for estimating prophylactic efficacy from these models [11, 12, 21–24, 28, 46, 47]. Essentially, to estimate prophylactic efficacy with stochastic simulation approaches, a large number of stochastic trajectories is sampled and subsequently classified into infection or extinction events to derive a sample statistic of, for example, the probability of infection $\hat{P}_I(Y_t, \mathcal{S})$. More recently, the extra reaction algorithm for networks in dynamic environments (EXTRANDE) [41] was adapted in [11] to couple pharmacokinetics with intrinsically stochastic viral dynamics following exposure, and to accurately classify stochastic trajectories. Despite the advantages of stochastic approaches, the disadvantages are also very clear: To obtain meaningful statistics, many stochastic simulations need to be conducted to accurately determine the *sample statistics* $\hat{P}_I(Y_t, \mathcal{S})$. The latter makes the stochastic methods expensive in terms of overall computational time, such that many important *in silico* experiments are infeasible. In particular, the scope of sensitivity analysis with regards to aforementioned factors in integrated, multiscale-models is usually limited. In this work, we introduce three low-dimensional approaches to estimate the prophylactic efficacy in considerably less time, in a single run. We envision that these approaches can greatly expand the scope of analysis with regards to estimating prophylactic efficacy, by allowing to analyse the long-term effect of prophylaxis, as well as performing sensitivity analysis.

Stochastic simulation methods sample trajectories of the whole system, where any state may arise during simulation. However, in the context of prophylaxis, one is only interested in the probabilities of extinction (and its complement, infection). Therefore, for each state, only those parts that contribute to the extinction event need to be considered. Because the probability of extinction for an arbitrary state can be expressed with the extinction probabilities of the respective unit vectors (eq (14); statistical independence), only extinction probabilities for unit vectors need to be computed. This is the main idea behind the three proposed low-dimensional Ansatz functions.

The first method (Next Transition Method (NTM)) is based on the embedded Markov chain described in [11]. The method was inspired by the idea that the probability distributions of state transitions $\mathrm{V} \to \mathrm{T}_1$, $\mathrm{T}_1 \to \mathrm{T}_2$ and $\mathrm{T}_2 \to \mathrm{T}_2 + \mathrm{V}$ can be determined, as shown in eqs. (16)– (18). Starting from the unit vector, this method considers all possible one-step transitions. We used three functions to denote a probability function, i.e. $d_1(t, i)$, $d_2(t, i)$ and $d_3(t, i)$. These functions represent the probability that the corresponding transition occurs in the discrete time interval $[t + (i-1) \cdot \Delta t, t + i \cdot \Delta t)$. The time-dependent functions ($d_2(t, i)$ in our case) are then approximated (zero order Taylor approximation) for small time spans Δt and the extinction probabilities are iteratively computed *backwards* in time using dynamic programming, as outlined in Supplementary Text S3.

The constant time step method (CTSM) is based on the discrete-time Markov chain of the underlying virus dynamics model. Similar to the NTM, the time was discretized into fixed time steps Δt for which the probability flux is computed (eqs. (24)–(26)). In this method, time-dependent functions, e.g. a_5, are approximated by a zero-order Taylor approximation for each time step Δt. Like NTM, the extinction probabilities are

bioRxiv preprint doi: https://doi.org/10.1101/2021.07.22.453374; this version posted July 22, 2021. The copyright holder for this preprint (which was not certified by peer review) is the author/funder, who has granted bioRxiv a license to display the preprint in perpetuity. It is made available under aCC-BY 4.0 International license.

iteratively computed *backwards* in time using dynamic programming, as outlined in Supplementary Text S4.

For both NTM and CTSM, Δt must be determined beforehand (see S2 Text and S3 Text). In CTSM, only the next time step Δt is considered, and no look-ahead horizons is needed, which makes the method more efficient than NTM (see Table 2). Compared to NTM, the implementation of CTSM is also simpler as only one time step must be considered in each iteration.

Lastly, the Probability Generating System (PGS), eq. (27) can easily be derived from the CTSM by replacing the constant time step Δt by an infinitesimally small step dt. The method is therefore based on a continuous-time Markov process. Because of the time continuity, the explicit approximations in NTM and CTSM are not necessary in the PGS. In our implementation of the method, we solved the pharmacokinetics beforehand and then wrapped the values of a_5 into a function that can be called directly from within the PGS's ODEs, which are solved *backwards in time*. It is notable that a backward ODE solver must be used in the implementation, and the use and configuration of different ODE solvers will have an impact on the accuracy and efficacy of this method. However, since modern ODE-solvers use adaptive step sizes, less computations may be needed to ensure accurate results, in comparison to a constant step size method (like NTM or CTSM), Table 2.

The set of ordinary differential equations (eq. (27)) derived for the PGS is related to the Kolmogorov backward equations [48], which was used in [22]. The major improvement of our work is to combine this Ansatz with the PK-PD profile of the prophylaxis (eq. (10)) so that the prophylactic efficacy can be computed with arbitrary prophylactic dosing schedules.

While the PGS is directly related to the CTSM, we show in Supplementary Text S6, how to derive PGS from the NTM. Hence, we demonstrated that the three proposed methods describe the same process, using different formalisms and approximations.

In Figure 3, we also compared the methods head-to-head to demonstrate the equivalence of the obtained results. Figure 3 also shows results of stochastic simulations with EXTRANDE, which delivers consistent, but less accurate results. Likewise, Table 3 shows the consistency of prediction with PGS and EXTRANDE, regarding the prophylactic efficacy for different DTG regimens with multiple viral exposures.

Using the proposed methods, we can also perform analyses that are computationally infeasible with stochastic simulations. As shown in Figure 5, the long-term prophylactic efficacy profiles were computed using PGS with four different values of adherence and a virtual patient cohort of 1000 individuals. This type of analysis allows to quantify sensitivity with regards to adherence and inter-individual pharmacokinetic variability. The analysis showed that DTG can protect highly adherent individuals from acquiring HIV infection and that inter-individual differences are most strongly affecting prophylaxis at times of inconsistent use of the prophylaxis. Moreover, when several consecutive pills are missed, prophylactic efficacy may drop below 50%. Interestingly, the long-term prophylactic efficacy computation took less than 2 seconds for one virtual patient. To compute the corresponding profile with EXTRANDE, for example if an efficacy estimate is to be computed for every hour using 5000 simulations, a total of $24 \times 365 \times 5000 \approx 44$ million simulations for a single adherence level would need to be conducted. Besides computational time, power consumption (and possible carbon imprint) could therefore be considerably reduced using the proposed methods.

Another possible application of the proposed methods is the possibility to estimate the time of the extinction event, Fig. 6. As a showcase of a sensitivity analysis, we estimated, for a 3-days 50mg DTG regimen, the probability density function of the extinction event, when a single, versus 20 viruses were initially reaching a replication-competent physiological compartment. The analysis showed that the time to

bioRxiv preprint doi: https://doi.org/10.1101/2021.07.22.453374; this version posted July 22, 2021. The copyright holder for this preprint (which was not certified by peer review) is the author/funder, who has granted bioRxiv a license to display the preprint in perpetuity. It is made available under aCC-BY 4.0 International license.

viral extinction is increased for larger inoculum sizes (more viruses). This analysis thus highlights the complex interplay between viral exposure and prophylaxis that can be analysed with the proposed methods and be used to optimize HIV prophylaxis. With regards to data, interestingly, in vaginal SHIV viral challenge models, which are typically conducted with large inoculum sizes, late viral breakthrough has been observed [49, 50].

The presented methods have been derived for the model depicted in Fig. 1 and need to be adjusted if other viral dynamics models were used. In Supplementary Text S5, we derive the three methods for an extended viral dynamics model that additionally considers long-lived cells (e.g. macrophages) and infected T cells, which may turn dormant, e.g. become latently infected. It is well established that these latent reservoirs are a major obstacle to the elimination of HIV during therapy [51]. While these reservoirs are established early in infection, it is unclear whether they alter prophylactic efficacy. To test this hypothesis, we used the proposed methods for the extended viral dynamic model (Supplementary Text S5). When comparing the results with those from the simpler model, we however found that the impact of the reservoirs on prophylactic efficacy was negligible.

In summary, we propose three novel methods that can estimate the efficacy of arbitrary prophylactic regimen and viral exposures within seconds. The three methods allow to integrate individual PK/PD profiles and viral dynamics into a single framework and they are more exact than state-of-art hybrid stochastic simulation schemes, like EXTRANDE. We envision that the new methods can be applied in many circumstances, in which the stochastic simulation is computationally infeasible, such as parameter sensitivity analysis or long-term efficacy estimation. To this end, the proposed methods may even be suitable as part of an App, which may help PrEP users to monitor and plan their PrEP regimen. Moreover, the general schemes may be adapted to study related biomedical questions, like prophylactic efficacy in other pathogens or vaccine efficacy.

bioRxiv preprint doi: https://doi.org/10.1101/2021.07.22.453374; this version posted July 22, 2021. The copyright holder for this preprint (which was not certified by peer review) is the author/funder, who has granted bioRxiv a license to display the preprint in perpetuity. It is made available under aCC-BY 4.0 International license.

Supporting information

S1 Text The supplementary text contains a supplementary derivations for all proposed methods (NTM, CTSM and PGS).

S2 Text The supplementary text contains a complete pseudo-code and the implementation details for the Next Transition Method (NTM).

S3 Text The supplementary text contains a complete pseudo-code and the implementation details for the Constant Time Step Method (CTSM).

S4 Text The supplementary text contains a complete pseudo-code and the implementation details for the Probability Generating System (PGS).

S5 Text The supplementary text entails the derivation of the equations for the NTM, CTSM and PGS for a extended viral dynamic model that contains long-lived and latently infected viral reservoirs.

S6 Text The supplementary text derived the Probability Generating System (PGS) from the Next Transition Method (NTM).

Acknowledgments

L.Z. and M.v.K. acknowledge funding from the German Ministry for Science and Education (BMBF; grant number 01KI2016). The funders had no role in designing the research or the decision to publish.

Author contributions

Conceptualization: L.Z. and M.v.K.; formal analysis: L.Z., J.W. and M.v.K.; funding acquisition: M.v.K.; methodology: L.Z. and J.W.; project administration: M.v.K.; software: L.Z. and J.W.; supervision: M.v.K; visualization: L.Z.; writing – original draft: L.Z. and M.v.K.; writing – review and editing: L.Z., J.W. and M.v.K..

Declaration of interests

The authors declare no competing interests.

References

1. Sharp PM, Hahn BH. Origins of HIV and the AIDS pandemic. Cold Spring Harbor Perspectives in Medicine. 2011;1(1):a006841.
2. UNAIDS. FACT SHEET – GLOBAL AIDS UPDATE 2020; 2020. https://www.unaids.org/en/resources/fact-sheet.
3. Stover J, Kelly SL, Mudimu E, Green D, Smith T, Taramusi I, et al. The Risks and Benefits of Providing HIV Services during the COVID-19 Pandemic. MedRXiV (https://doiorg/101101/2021030121252663). 2021;.

bioRxiv preprint doi: https://doi.org/10.1101/2021.07.22.453374; this version posted July 22, 2021. The copyright holder for this preprint (which was not certified by peer review) is the author/funder, who has granted bioRxiv a license to display the preprint in perpetuity. It is made available under aCC-BY 4.0 International license.

4. Gulick RM. Investigational Antiretroviral Drugs: What is Coming Down the Pipeline. Top Antivir Med. 2018;25(4):127–132.

5. Trono D, Van Lint C, Rouzioux C, Verdin E, Barré-Sinoussi F, Chun TW, et al. HIV persistence and the prospect of long-term drug-free remissions for HIV-infected individuals. Science. 2010;329(5988):174–80. doi:10.1126/science.1191047.

6. Archin NM, Sung JM, Garrido C, Soriano-Sarabia N, Margolis DM. Eradicating HIV-1 infection: seeking to clear a persistent pathogen. Nat Rev Microbiol. 2014;12(11):750–64. doi:10.1038/nrmicro3352.

7. Caskey M, Klein F, Nussenzweig MC. Broadly neutralizing anti-HIV-1 monoclonal antibodies in the clinic. Nat Med. 2019;25(4):547–553. doi:10.1038/s41591-019-0412-8.

8. Cohen MS, Smith MK, Muessig KE, Hallett TB, Powers KA, Kashuba AD. Antiretroviral treatment of HIV-1 prevents transmission of HIV-1: where do we go from here? The Lancet. 2013;382(9903):1515–1524.

9. Grant RM, Lama JR, Anderson PL, McMahan V, Liu AY, Vargas L, et al. Preexposure chemoprophylaxis for HIV prevention in men who have sex with men. N Engl J Med. 2010;363(27):2587–99. doi:10.1056/NEJMoa1011205.

10. Mayer KH, Molina JM, Thompson MA, Anderson PL, Mounzer KC, De Wet JJ, et al. Emtricitabine and tenofovir alafenamide vs emtricitabine and tenofovir disoproxil fumarate for HIV pre-exposure prophylaxis (DISCOVER): primary results from a randomised, double-blind, multicentre, active-controlled, phase 3, non-inferiority trial. Lancet. 2020;396(10246):239–254. doi:10.1016/S0140-6736(20)31065-5.

11. Duwal S, Dickinson L, Khoo S, von Kleist M. Hybrid stochastic framework predicts efficacy of prophylaxis against HIV: An example with different dolutegravir prophylaxis schemes. PLOS Computational Biology. 2018;14(6):e1006155.

12. Duwal S, Seeler D, Dickinson L, Khoo S, von Kleist M. The Utility of Efavirenz-based Prophylaxis Against HIV Infection. A Systems Pharmacological Analysis. Front Pharmacol. 2019;10:199. doi:10.3389/fphar.2019.00199.

13. Pipeline AR. `https://www.prepwatch.org/nextgen-prep/research-pipeline/`;.

14. Flexner C, Owen A, Siccardi M, Swindells S. Long-acting drugs and formulations for the treatment and prevention of HIV infection. Int J Antimicrob Agents. 2021;57(1):106220. doi:10.1016/j.ijantimicag.2020.106220.

15. Coelho LE, Torres TS, Veloso VG, Landovitz RJ, Grinsztejn B. Pre-exposure prophylaxis 2.0: new drugs and technologies in the pipeline. The Lancet HIV. 2019;6(11):e788–e799.

16. Royce RA, Seña A, Cates W Jr, Cohen MS. Sexual transmission of HIV. N Engl J Med. 1997;336(15):1072–8. doi:10.1056/NEJM199704103361507.

17. Dunn DT, Glidden DV. Statistical issues in trials of preexposure prophylaxis. Curr Opin HIV AIDS. 2016;11(1):116–21. doi:10.1097/COH.0000000000000218.

bioRxiv preprint doi: https://doi.org/10.1101/2021.07.22.453374; this version posted July 22, 2021. The copyright holder for this preprint (which was not certified by peer review) is the author/funder, who has granted bioRxiv a license to display the preprint in perpetuity. It is made available under aCC-BY 4.0 International license.

18. Hendrix CW. HIV Antiretroviral Pre-Exposure Prophylaxis: Development Challenges and Pipeline Promise. Clin Pharmacol Ther. 2018;104(6):1082–1097. doi:10.1002/cpt.1227.

19. Joseph SB, Swanstrom R, Kashuba ADM, Cohen MS. Bottlenecks in HIV-1 transmission: insights from the study of founder viruses. Nat Rev Microbiol. 2015;13(7):414–25. doi:10.1038/nrmicro3471.

20. Czuppon P, Débarre F, Gonçalves A, Tenaillon O, Perelson AS, Guedj J, et al. Success of prophylactic antiviral therapy for SARS-CoV-2: Predicted critical efficacies and impact of different drug-specific mechanisms of action. PLoS Comput Biol. 2021;17(3):e1008752. doi:10.1371/journal.pcbi.1008752.

21. Duwal S, Dickinson L, Khoo S, von Kleist M. Mechanistic framework predicts drug-class specific utility of antiretrovirals for HIV prophylaxis. PLoS Comput Biol. 2019;15(1):e1006740. doi:10.1371/journal.pcbi.1006740.

22. Conway JM, Konrad BP, Coombs D. Stochastic analysis of pre-and postexposure prophylaxis against HIV infection. SIAM Journal on Applied Mathematics. 2013;73(2):904–928.

23. Duwal S, Schütte C, von Kleist M. Pharmacokinetics and pharmacodynamics of the reverse transcriptase inhibitor tenofovir and prophylactic efficacy against HIV-1 infection. PLoS One. 2012;7(7):e40382. doi:10.1371/journal.pone.0040382.

24. Duwal S, Sunkara V, von Kleist M. Multiscale Systems-Pharmacology Pipeline to Assess the Prophylactic Efficacy of NRTIs Against HIV-1. CPT Pharmacometrics Syst Pharmacol. 2016;5(7):377–87. doi:10.1002/psp4.12095.

25. van der Toorn W, Oh DY, von Kleist M, working group on SARS-CoV-2 Diagnostics at RKI. COVIDStrategyCalculator: A software to assess testing- and quarantine strategies for incoming travelers, contact person management and de-isolation. Patterns (N Y). 2021; p. 100264. doi:10.1016/j.patter.2021.100264.

26. Von Kleist M, Menz S, Huisinga W. Drug-class specific impact of antivirals on the reproductive capacity of HIV. PLOS Computational Biology. 2010;6(3):e1000720.

27. von Kleist M, Menz S, Stocker H, Arasteh K, Schütte C, Huisinga W. HIV quasispecies dynamics during pro-active treatment switching: impact on multi-drug resistance and resistance archiving in latent reservoirs. PlOS ONE. 2011;6(3):e18204.

28. Tuckwell HC, Shipman PD, Perelson AS. The probability of HIV infection in a new host and its reduction with microbicides. Mathematical Biosciences. 2008;214(1-2):81–86.

29. Tan WY, Wu H. Stochastic modeling of the dynamics of CD4+ T-cell infection by HIV and some Monte Carlo studies. Mathematical Biosciences. 1998;147(2):173–205.

30. Pierson TC, Zhou Y, Kieffer TL, Ruff CT, Buck C, Siliciano RF. Molecular characterization of preintegration latency in human immunodeficiency virus type 1 infection. Journal of virology. 2002;76(17):8518–8531.

31. Zhou Y, Zhang H, Siliciano JD, Siliciano RF. Kinetics of human immunodeficiency virus type 1 decay following entry into resting CD4+ T cells. Journal of Virology. 2005;79(4):2199–2210.

bioRxiv preprint doi: https://doi.org/10.1101/2021.07.22.453374; this version posted July 22, 2021. The copyright holder for this preprint (which was not certified by peer review) is the author/funder, who has granted bioRxiv a license to display the preprint in perpetuity. It is made available under aCC-BY 4.0 International license.

32. Sedaghat AR, Dinoso JB, Shen L, Wilke CO, Siliciano RF. Decay dynamics of HIV-1 depend on the inhibited stages of the viral life cycle. Proceedings of the National Academy of Sciences. 2008;105(12):4832–4837.

33. Wei X, Ghosh SK, Taylor ME, Johnson VA, Emini EA, Deutsch P, et al. Viral dynamics in human immunodeficiency virus type 1 infection. Nature. 1995;373(6510):117–122.

34. Sedaghat AR, Siliciano RF, Wilke CO. Constraints on the dominant mechanism for HIV viral dynamics in patients on raltegravir. Antiviral Therapy. 2009;14(2):263.

35. Koelsch KK, Liu L, Haubrich R, May S, Havlir D, Günthard HF, et al. Dynamics of total, linear nonintegrated, and integrated HIV-1 DNA in vivo and in vitro. The Journal of Infectious Diseases. 2008;197(3):411–419.

36. Markowitz M, Louie M, Hurley A, Sun E, Di Mascio M, Perelson AS, et al. A novel antiviral intervention results in more accurate assessment of human immunodeficiency virus type 1 replication dynamics and T-cell decay in vivo. Journal of Virology. 2003;77(8):5037–5038.

37. Chou TC. Theoretical basis, experimental design, and computerized simulation of synergism and antagonism in drug combination studies. Pharmacological Reviews. 2006;58(3):621–681.

38. Duwal S, Dickinson L, Khoo S, von Kleist M. Mechanistic framework predicts drug-class specific utility of antiretrovirals for HIV prophylaxis. PLOS Computational Biology. 2019;15(1):e1006740.

39. Wilkinson DJ. Stochastic modelling for systems biology. CRC press; 2018.

40. SciPy; 2021. `https://docs.scipy.org/doc/scipy/reference/generated/scipy.integrate.solve_ivp.html`.

41. Voliotis M, Thomas P, Grima R, Bowsher CG. Stochastic simulation of biomolecular networks in dynamic environments. PLOS Computational Biology. 2016;12(6):e1004923.

42. Greenwood M, et al. A report on the natural duration of cancer. A Report on the Natural Duration of Cancer. 1926;(33).

43. Shen L, Peterson S, Sedaghat AR, McMahon MA, Callender M, Zhang H, et al. Dose-response curve slope sets class-specific limits on inhibitory potential of anti-HIV drugs. Nat Med. 2008;14(7):762–6. doi:10.1038/nm1777.

44. Hatziioannou T, Evans DT. Animal models for HIV/AIDS research. Nat Rev Microbiol. 2012;10(12):852–67. doi:10.1038/nrmicro2911.

45. Cottrell ML, Yang KH, Prince HMA, Sykes C, White N, Malone S, et al. A Translational Pharmacology Approach to Predicting Outcomes of Preexposure Prophylaxis Against HIV in Men and Women Using Tenofovir Disoproxil Fumarate With or Without Emtricitabine. J Infect Dis. 2016;214(1):55–64. doi:10.1093/infdis/jiw077.

46. Bershteyn A, Eckhoff PA. A model of HIV drug resistance driven by heterogeneities in host immunity and adherence patterns. BMC Syst Biol. 2013;7:11. doi:10.1186/1752-0509-7-11.

bioRxiv preprint doi: https://doi.org/10.1101/2021.07.22.453374; this version posted July 22, 2021. The copyright holder for this preprint (which was not certified by peer review) is the author/funder, who has granted bioRxiv a license to display the preprint in perpetuity. It is made available under aCC-BY 4.0 International license.

47. Frank M, von Kleist M, Kunz A, Harms G, Schütte C, Kloft C. Quantifying the impact of nevirapine-based prophylaxis strategies to prevent mother-to-child transmission of HIV-1: a combined pharmacokinetic, pharmacodynamic, and viral dynamic analysis to predict clinical outcomes. Antimicrob Agents Chemother. 2011;55(12):5529–40. doi:10.1128/AAC.00741-11.

48. Kolmogoroff A. Über die analytischen Methoden in der Wahrscheinlichkeitsrechnung. Mathematische Annalen. 1931;104:415–458.

49. Andrews CD, Yueh YL, Spreen WR, Bernard LS, Boente-Carrera M, Rodriguez K, et al. A long-acting integrase inhibitor protects female macaques from repeated high-dose intravaginal SHIV challenge. Science translational medicine. 2015;7(270):270ra4–270ra4.

50. Kovarova M, Council OD, Date AA, Long JM, Nochii T, Belshan M, et al. Nanoformulations of rilpivirine for topical pericoital and systemic coitus-independent administration efficiently prevent HIV transmission. PLoS Pathog. 2015;11(8):e1005075.

51. Chun TW, Moir S, Fauci AS. HIV reservoirs as obstacles and opportunities for an HIV cure. Nature immunology. 2015;16(6):584–589.